

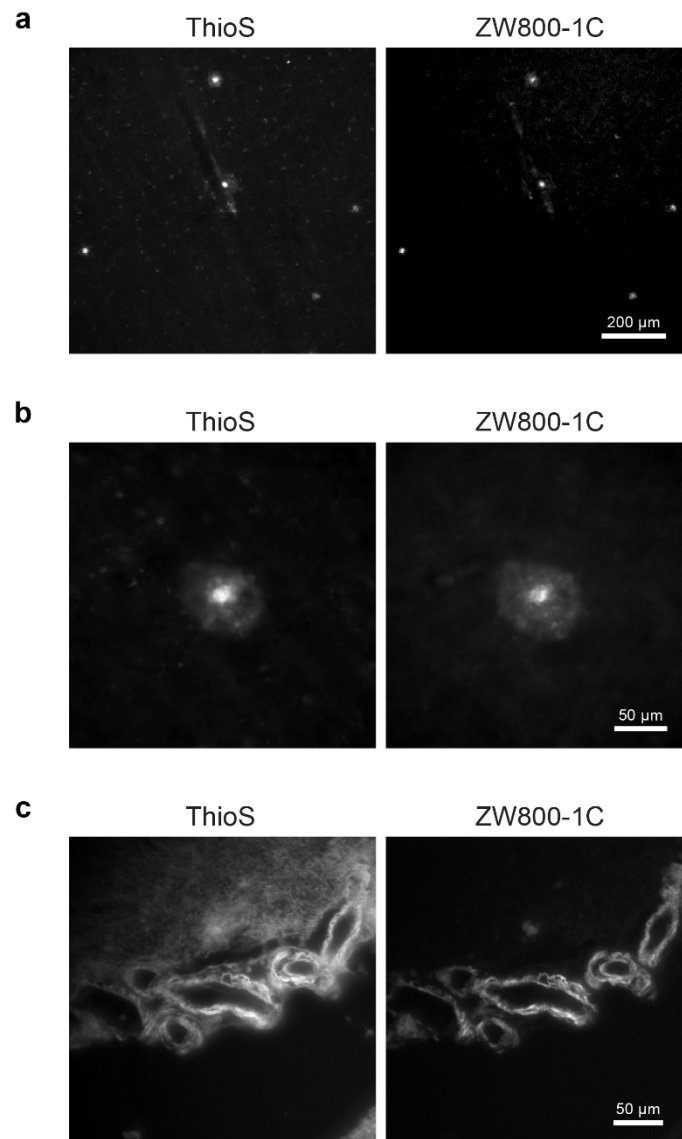
---

# Near-infrared fluorescence lifetime imaging of amyloid- $\beta$ aggregates and tau fibrils through the intact skull of mice

---

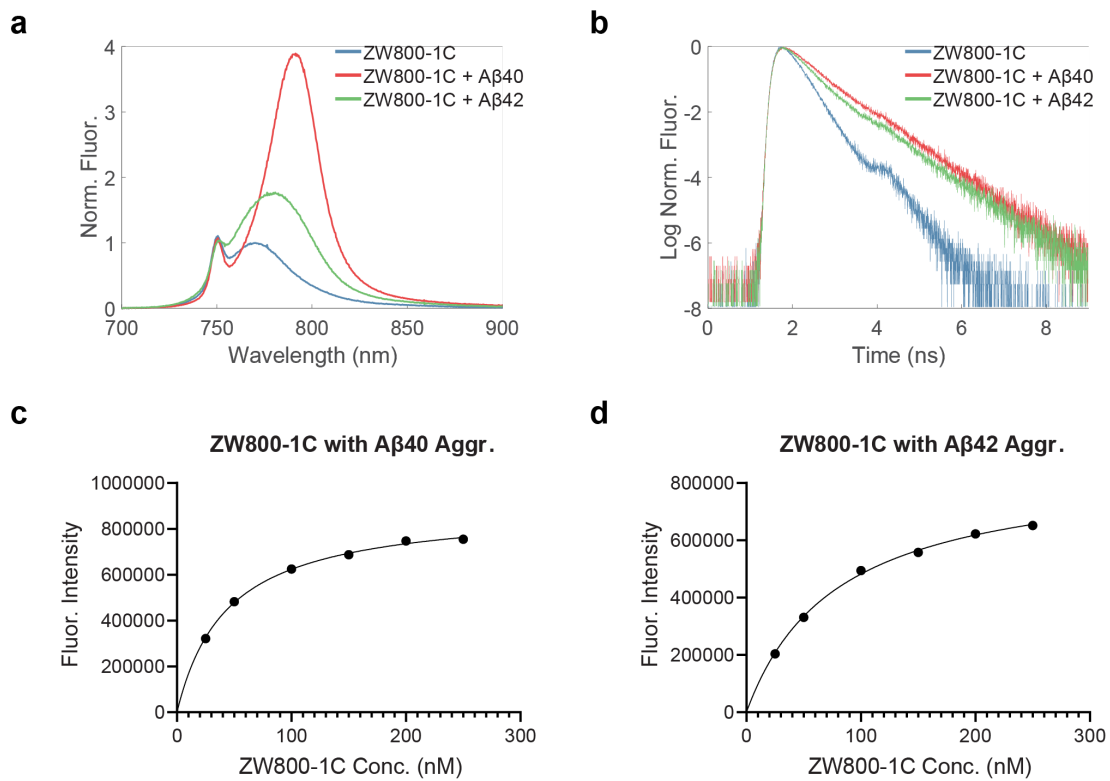
In the format provided by the authors and unedited

---



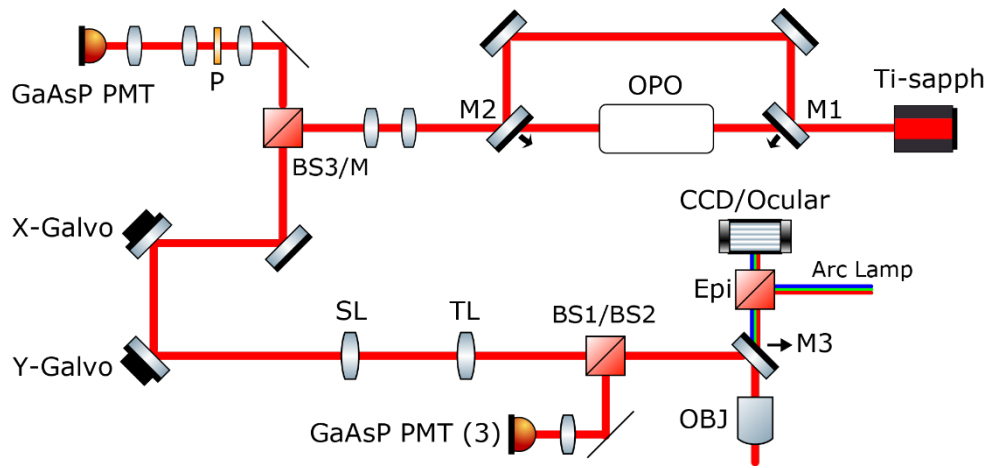
**Supplementary Fig. 1 | Ex vivo imaging to validate ZW800-1C binding of human AD pathology.**

Representative images show co-staining of (a) amyloid plaques at low magnification, (b) single plaque at high magnification, and (c) CAA with ThioS (0.05%) and ZW800-1C (100 μM) in human AD sections. Images were acquired with widefield epifluorescence imaging in the green and NIR channels.

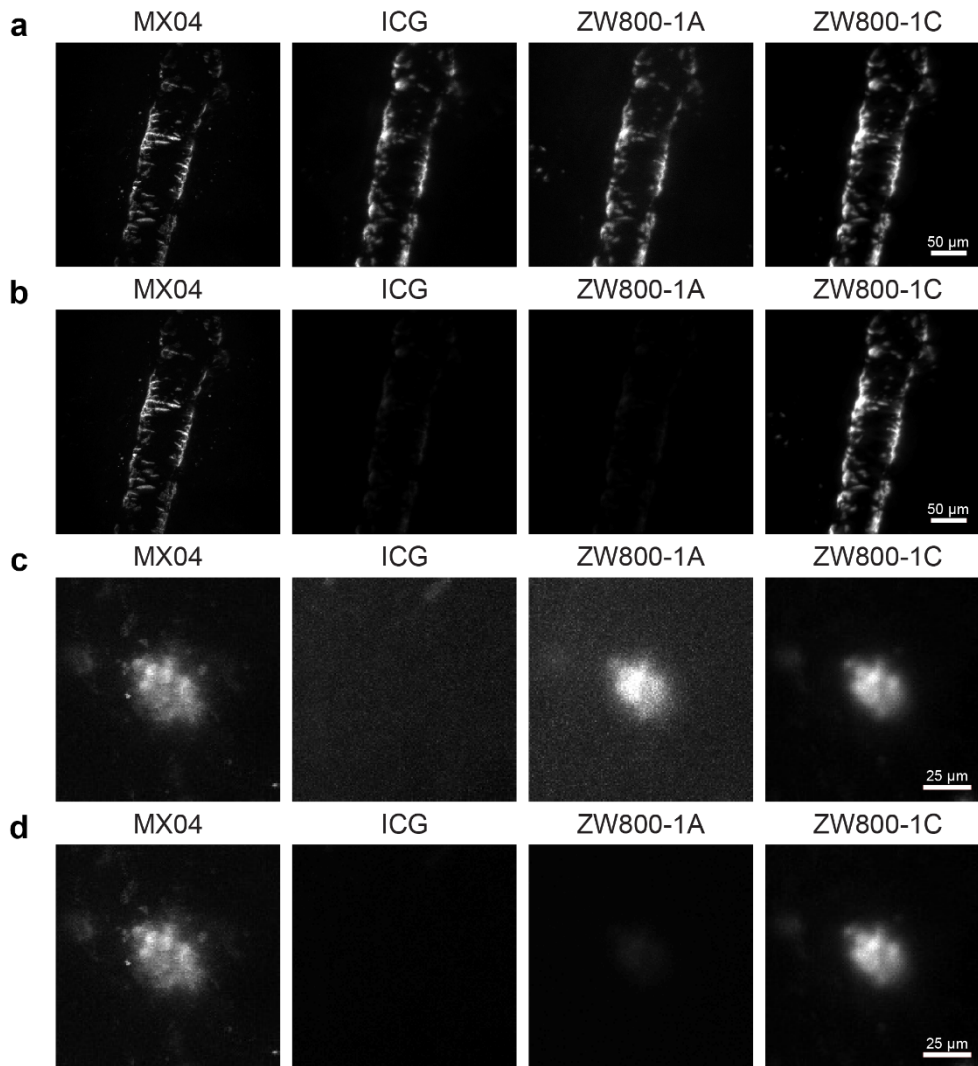


**Supplementary Fig. 2 | *In vitro* binding assays with ZW800-1C and amyloid- $\beta$  aggregates. (a)**

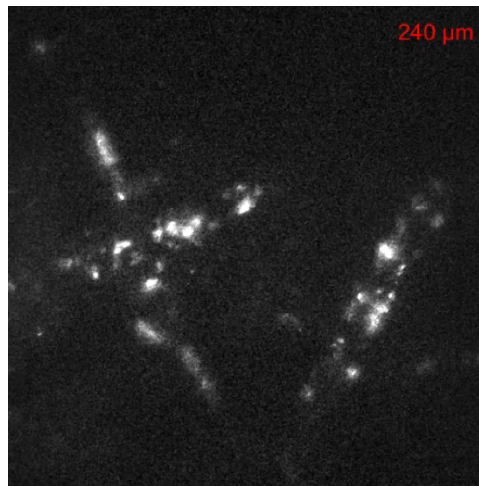
Fluorescence emission spectrum and (b) fluorescence decay curve of ZW800-1C alone in PBS (blue) and after mixing with with A $\beta$ 40 aggregates (red) and A $\beta$ 42 aggregates (green). The excitation peak at 750 nm is visible in the fluorescence emission spectra curves. Binding affinity measurement using varying concentrations of ZW800-1C mixed with (c) 500 nM A $\beta$ 40 aggregates and (d) 500 nM A $\beta$ 42 aggregates for the calculation of  $K_D$ .



**Supplementary Fig. 3 | Schematic for custom multimodal microscope system.** Two flip mirrors (M1 and M2) allow laser input from either the Ti-Sapph or the Ti-Sapph pumped OPO. Laser beams are expanded to ~5 mm and scanned using resonant and galvanometer scanners. The scan lens (SL) and tube lens (TL) are used to project the beam exiting the resonant/galvanometer scanners to the back aperture of the objective (OBJ). During confocal imaging, fluorescence is directed through a 100  $\mu\text{m}$  pinhole (P). The translatable mirror (M3) switches between multiphoton/confocal imaging and epifluorescence imaging with CCD/oculars. Beam splitters (BS), BS1 (700LP)/BS2 (965LP), and BS3 (810LP) are used to split excitation/fluorescence for multiphoton and confocal imaging, respectively.



**Supplementary Fig. 4 | Comparison between the labeling intensity of candidate NIR fluorophores when bound to the same amyloid plaque and CAA segment.** Single CAA segment and amyloid plaque are imaged after sequential intravenous injection (50 nmol) of ICG, ZW800-1A, and ZW800-1C in the same Tg APP/PS1 mouse. For all measurements, any previous injection of NIR fluorophore is confirmed to no longer be detectable in the brain before another injection is performed. MX04 is intraperitoneally injected to co-label amyloid- $\beta$  aggregates. In rows (a) and (c), the NIR images are independently normalized to reveal weaker intensity values, while in rows (b) and (d), the NIR images are normalized to the same intensity value based on the brightest image (ZW800-1C in both cases) so that relative intensity differences among the NIR fluorophores can be directly compared.



**Supplementary Video 1 | *In vivo* through the skull imaging of APP/PS1 mouse.** Using multiphoton microscopy, 3D volume was acquired through the intact skull of a 9-month-old APP/PS1 mouse. 100 nmol of ZW800-1C was injected intravenously 2 h prior to imaging. The excitation laser was set to 1,300 nm, and fluorescence emission was collected from 750 nm to 830 nm.